

Model Calculations about the Influence of Protic Environments on the Alkylation Step of Epoxide, Aziridine, and Thiirane Based Cysteine Protease Inhibitors

Holger Helten,[†] Tanja Schirmeister,[‡] and Bernd Engels^{*,†}

Institut für Organische Chemie, and Institut für Pharmazie und Lebensmittelchemie,
Universität Würzburg, Am Hubland, D-97074 Würzburg, Germany

Received: March 18, 2004; In Final Form: July 13, 2004

Cysteine proteases play pivotal roles in many diseases, making them attractive targets for the development of new drugs. Prominent lead structures for irreversible inhibitors of these enzymes are peptides and peptidomimetics containing the three-membered heterocycles epoxide, aziridine, or thiirane as electrophilic warheads. Until now, no systematic study has been performed to analyze the inherent different inhibition potencies of the three inhibitor types (epoxide, aziridine, thiirane) as well as their different inhibition behavior in dependence of the environment (e.g., pH dependency of inhibition). This is the goal of the present study. By analyzing the computed energy profiles of appropriate model reactions, we investigate to what extent a decreasing pH value changes the mechanisms, the thermodynamics, and kinetics of the irreversible inhibition step. Besides the energies, changes in the geometrical arrangements of the systems are also studied. Additionally, possible influences of entropy effects are estimated and the accuracy of the theoretical approaches is assessed. Our results show that the large enhancement of the inhibition potencies of aziridines at lower pH values results from a strong catalysis even by weak proton donors. For epoxides and thiiranes much lower effects are found.

Introduction

Cysteine proteases play pivotal roles in many diseases making them attractive targets for the development of new drugs.¹ A typical irreversible cysteine protease inhibitor consists of an electrophilic building block (e.g., epoxide ring) attached to a peptidic or peptidomimetic sequence (Figure 1). [For reviews, see refs 1c, 1d and 2.]

Epoxysuccinyl peptides like E-64c (=EP-475) and E-64d (ethyl ester of EP-475)¹⁸ (Figure 1) are one of the best-studied inhibitor classes. They are derived from the natural compound E-64 ((*S,S*)-1-[*N*-[[(*L*-3-*trans*-carboxyoxiran-2-yl)carbonyl]-*L*-leucyl]amino]-4-guanidinobutane) isolated from *Aspergillus japonicus*.³ The success of this compound class as selective, highly potent and irreversible cysteine protease inhibitors (“quiescent affinity labels”) has led to syntheses and evaluation of analogous peptides containing other electrophilic three-membered (hetero)cycles: aziridines,⁴ thiiranes,⁵ and cyclopropanes.⁶

The kinetic and thermodynamic data characterizing irreversible enzyme inhibition by such inhibitors are derived from the following minimal two-step mechanism:



First, in a reversible reaction a noncovalent enzyme inhibitor complex (EI) is formed. In the second, rate-determining step, described by the first-order rate constant of inhibition k_i , the negatively charged active site's thiolate attacks the electrophilic three-membered ring. The following irreversible ring-opening

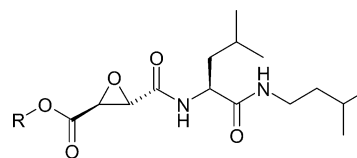


Figure 1. Epoxysuccinyl derived cysteine protease inhibitors.

reaction leads to an alkylation of the active site cysteine residue resulting in a covalently modified and inactivated enzyme (E–I) (Figure 2). This second alkylation step is affected by the kinetics and thermodynamics of the ring opening. The second-order rate constant of inhibition (defined as $k_{\text{second}} = k_i/K_i$) describes the overall inhibition potency of irreversible inhibitors. For epoxide based inhibitors the influence of the substitution pattern of the three membered rings on the rate of inactivation was investigated in several studies,^{7–9} but an experimental differentiation between the influence on the reversible and the irreversible step was seldom performed.

Such a differentiation was done by Meara and Rich,⁷ who found that the replacement of the R = CO₂H substituent of the epoxide ring of EP-475 (Figure 1) by R = CONHOH, CONH₂, or COCH₃ changed the first-order rate of inhibition k_i only slightly. Only the substituents R = CO₂CH₂CH₃ and CH₂OH reduced k_i by about one order of magnitude. This finding is in contrast to pseudo-first-order rates of the reaction of methylthiolate with α,β -epoxy carbonyl compounds¹⁰ at alkaline pH; for these systems the rates of attack by a thiolate on the α -carbon decreased by 3 orders of magnitude in the order ketone > amide > acid.

Beside the properties of the electrophilic warhead, the proteinic or physiological environment is also expected to be

* Corresponding author. Fax: +49 (0)931/888 5331. E-mail: engels@chemie.uni-wuerzburg.de.

[†] Institut für Organische Chemie, Universität Würzburg.

[‡] Institut für Pharmazie und Lebensmittelchemie, Universität Würzburg.

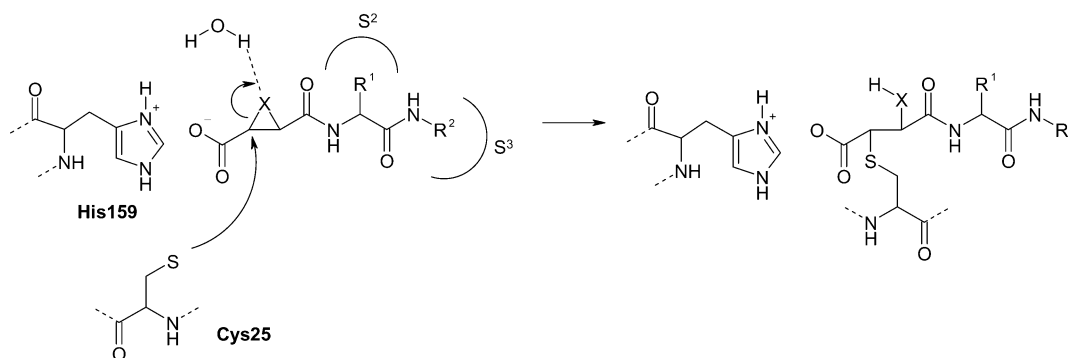


Figure 2. Proposed inhibition mechanism of cysteine protease inhibitors containing three-membered heterocycles attached to a peptidic/peptidomimetic chain. (His159, Cys25: active site diad, papain numbering).

important for this second step. For example, for epoxide based inhibitors it has been postulated that during the inactivation of papain the epoxide moiety would be protonated by His159.¹¹ On the basis of the crystal structure of papain alkylated by E-64, Varughese et al. argued that the epoxide was more likely protonated by water (Figure 2) because of the distance of the resulting hydroxyl from His159.^{12a} This finding was supported by Meara and Rich,⁷ who investigated the pH-dependency of the inhibition of papain by the carboxamide analogue of EP-475. They did not find an alkaline pH dependency for the inhibition of papain by the above-mentioned inhibitor. Furthermore, the association process was found to be completely pH independent while at pH ≈ 3 the k_i value ($\log k_i \approx -1.5$) was 1–2 orders of magnitude lower compared to pH ≥ 5 . It was postulated that this pH dependency results from a protonation of an acidic group possessing a pK_a value around 4. On the basis of the behavior in the alkaline pH region, a water molecule was postulated as the most probable proton source.

Another example for the influence of the environment on the inhibition is the dependency of the second-order rate constant of inhibition $k_{\text{second}} = k_i/K_i$ of aziridine-2,3-dicarboxylic acid derived cysteine protease inhibitors on the pH value. For pH values around 7 the inhibition data reveal lower k_{second} values than for the epoxides, but for pH values around 4, *N*-unsubstituted and *N*-alkylated aziridines are as potent as epoxides.^{4b,c,d} *N*-Acylated ones show the same pH-dependency of inhibition as the epoxides, namely a pH optimum for inhibition around pH 6–7.^{4b,c}

A direct comparison to thiiranes is only possible between aziridine-2-carboxylic acid derivatives^{4e,13} and corresponding thiiranes⁵ (e.g., (*S*)-aziridine-2-carboxylic acid. $k_{\text{second}} = 1020 \text{ M}^{-1} \text{ min}^{-1}$;¹³ (*S*)-thiirane-2-carboxylic acid. $k_{\text{second}} = 222 \text{ M}^{-1} \text{ min}^{-1}$).⁵ These data show that thiiranes are less potent than the corresponding aziridines.

The inhibition properties of the three inhibitor types (epoxide, aziridine, thiirane) will be influenced from all parts of the enzyme–inhibitor system (inhibitor structure, active site, protein and physiological environment). Calculations can provide insights into the impact of the single components on the complete system and can compare the reaction mechanism of the various aforementioned cysteine protease inhibitors. However, there are only various theoretical studies which investigated ring opening reactions induced by other nucleophiles than thiolates. Lau et al.¹⁴ and Laitinen et al.¹⁵ modeled the noncatalyzed and the acid-catalyzed ring opening reaction of oxirane by the nucleophilic addition of acetate. In both studies, the gas-phase reactions were compared with the reactions in a polar solvent. The gas-phase reactions of oxiranes with nucleophiles were computed by Glad and Jensen,¹⁶ Gronert and Lee,¹⁷ and Omoto and Fujimoto.¹⁸ The latter modeled the influence

of bidentate acids but did not include bulk effects of a polar solvent. Gronert and Lee¹⁷ compared the ring opening reactions of oxirane and thiirane. The gas-phase ring opening of thiirane with ammonia and amines were computed by Banks and White.¹⁹ Various aziridines were compared in an ab initio study of Nielsen²⁰ who focused on the nitrogen inversion, the thermochemistry and the ring opening resulting from an unimolecular isomerization. Finally, various contributors to the rate enhancement in gas-phase nucleophilic strain releasing reactions of cyclic ring systems containing O, N, or S were studied by Wolk et al.²¹

Goal and Theoretical Approach of the Present Work

Since related studies are missing, we decided to perform an investigation with the general aim to elucidate the impact of the various parts of the total system onto the inhibition mechanisms of the three aforementioned inhibitor types. In the present study we focus on the question whether the different pH dependencies of the inhibition potency of epoxides and aziridines are related to kinetics and thermodynamics of the irreversible alkylation step. Relevant information is obtained by computing the reaction profiles of the ring opening of epoxides, aziridines and thiiranes for different environments using quantum chemical approaches.

In our model system, the attacking cysteine is mimicked by a methyl thiolate ($\text{H}_3\text{C}-\text{S}^-$) while the inhibitors are modeled by the three membered ring systems $(\text{H}_2\text{C})_2\text{X}$ with $\text{X} = \text{O}, \text{NH}, \text{S}$. Our model captures the effect of a decreasing pH value on the reaction profile by a series of model systems in which solvent molecules with increasing proton donor ability are placed in the vicinity of the heteroatom of the three membered rings and in the vicinity of the methyl thiolate. Water molecules were employed to mimic environments with weak proton donor ability ($pK_a = 15.74$), while NH_4^+ ($pK_a \approx 9.3$) and HCO_2H ($pK_a \approx 3.8$) molecules were used to simulate environments with higher proton donor abilities. The influence of the changing environment is always mimicked in two ways. In the first model a proton donor (e.g., NH_4^+) is placed in the vicinity of the heteroatom of the three-membered ring while a water molecule is positioned around the methyl thiolate. In the second model, a second proton donor replaces this water molecule. The latter computations also include effects that arise if the reactivity of the attacking methyl thiolate unit is weakened due to the increasing proton donor ability of the environment. Both models are of interest since the attacking cysteine unit is localized deeper inside the enzyme than the inhibitor, i.e., the latter is more exposed to the acid environment as shown by X-ray crystallography of cysteine proteases.¹² Consequently, a decreasing pH value (increasing proton donor ability) will influence the inhibitor more likely than the attacking cysteine.

TABLE 1: Influence of the Proton Donor Ability of the Environment on the Reaction Profiles of the Ring Opening Reactions^a

	solvent molecule	epoxide			aziridine				thiirane		
		TS	P	PH	TS	TSH	P	PH	TS	P	PH
entry 1	gas phase	+1.6	-16.9		+14.4		+6.0		-6.7 ^b	-26.9	
entry 2	- /- -	+16.9	-12.7		+30.2		+11.4		+10.9	-17.3	
entry 3	H ₂ O/- -	+14.4	-18.7		+28.4			-7.8	+9.9	-19.1	
entry 4	H ₂ O/H ₂ O	+14.4	-17.2	-26.0 ^c	+28.3			-6.1	+10.0	-17.6	
entry 5	NH ₄ ⁺ /H ₂ O	+11.8		-35.8		+12.9		-27.3	+8.5	-20.4	-19.0
entry 6	NH ₄ ⁺ /NH ₄ ⁺	+13.3		-32.4		+14.4		-23.8	+9.9	-17.2	-15.5
entry 7	HCO ₂ H/H ₂ O	+11.9		-37.7		+14.1		-25.4	+9.3	-19.3	-20.6
entry 8	HCO ₂ H/HCO ₂ ^{-d}	+17.0		-33.1		+20.0		-20.8	+15.2	-14.7	-15.9
entry 9	HCO ₂ H/HCO ₂ H ^e	+12.1		-35.9		+14.3		-23.7	+9.6	-17.5	-18.7

^a All energy values are relative to the reactants (kcal mol⁻¹). For more information, see text. ^b Optimized with B3LYP since with BLYP no TS could be located (see Table 3). ^c Computed with the standard GAUSSIAN settings for the COSMO approach, geometries not fully optimized. ^d Reactants: HCO₂⁻ + H₃CSH. ^e Reactants: HCO₂H + H₃CS⁻.

The paper is organized as follows: The first paragraph discusses the influence of various environments on the reaction profiles of the ring opening of epoxides, aziridines and thiiranes with methyl thiolate. In the second paragraph the size of entropy effects is estimated. The accuracy of the theoretical approach is assessed in the last paragraph.

Comparison of the Ring Opening Reactions in Environments with Increasing Proton Donor Ability

The computational results are summarized in Table 1, which contains the relative energies with respect to the reactants (kcal mol⁻¹). It contains electronic energies instead of free energies since the entropy effects (see below) of the present model reactions are more connected with the first reversible step of the inhibition mechanism than with the second, irreversible one, which is the topic of the present work. In Table 1, TS and P denote the transition states and the products, respectively. With increasing proton donor strength of the solvent molecules a proton transfer from the respective solvent molecule to the reacting species is predicted. This is indicated by the abbreviation PH for protonated products or TSH for protonated transition states. In all computations except for the gas-phase reactions the COSMO approach (standard parameters of the TURBO-MOLE program package)²² with $\epsilon = 78.39$ was employed to account for bulk effects of the polar physiological environment. Since computations with ϵ values of around 40 gave very similar results they are not listed. A visualization of some data of Table 1 is given in Figure 3. The geometrical arrangements found for the transition states and products of some selected model systems can be taken from Figures 4–8. For the epoxide as reactant we computed $R_{CC} = 1.47$ Å, $R_{CO} = 1.47$ Å, and $\angle CCO = 59.9^\circ$ while for the aziridine the values $R_{CC} = 1.49$ Å, $R_{CN} = 1.50$ Å, and $\angle CCN = 60.2^\circ$ were obtained. For the thiirane as reactant, the computations predicted $R_{CC} = 1.48$ Å, $R_{CS} = 1.88$ Å, and $\angle CCS = 66.8^\circ$. All geometrical parameters are summarized in the Supporting Information. The geometrical parameters of the stationary points were computed with the BLYP functional²³ in combination with the TZV+P basis sets²⁴ including the reaction field of the COSMO approach. The nature of the stationary points was checked by frequencies calculations. The relative energies were obtained from single point computations employing the B3LYP functional in combination with the same basis set. A discussion about the accuracy of this approach is given in the last paragraph.

The molecules included to mimic increasing proton donor ability of the surroundings are denoted in column 2 of Table 1. For example, NH₄⁺/H₂O (entry 5 of Table 1) indicates that one NH₄⁺ molecule was placed in the vicinity of the heteroatom of

the three membered ring and one water molecule in the neighborhood of the sulfur center of the attacking methyl thiolate. The geometries of these solvent molecules were explicitly optimized for the various stationary points of the reaction path. The abbreviation - /- - denotes that only the bulk effects of water as polar solvent were taken into account, while H₂O/- - indicates that only one water molecule was placed in the vicinity of the heteroatom of the heterocycle.

In the gas phase (energies in entry 1 of Table 1, Figure 3A, geometrical arrangements in Figure 4), the epoxide and the aziridine system possess small barriers. For the thiirane the TS is even more stable than the reactants. Such behavior is quite common for ion–neutral gas-phase reactions and arises because the charge of the reactants (methyl thiolate) becomes more delocalized during the reaction.^{14,16,18} As published for the gas-phase reaction of epoxides with acetate,^{14,15} low-energy ion–molecule-complexes (IMC) are also found for the present ring opening reactions. These IMCs are not given in Table 1 since they are strongly destabilized by polar solvents and are therefore unimportant for the present investigation. For the gas-phase ring opening reactions the order ΔE^\ddagger (thiirane) < ΔE^\ddagger (epoxide) << ΔE^\ddagger (aziridine) is predicted regarding the reaction barriers; i.e., the thiirane ring opening should be considerably faster than the epoxide one, and both should be much faster than the aziridine reaction. Concerning the thermodynamics, we find the aziridine reaction to be endothermic while for epoxide and thiirane exothermic gas-phase reactions are predicted, i.e., for the thermodynamics the same trend is found as for the reaction barriers (Figure 3A).

As already published for various reactions of epoxides with nucleophiles the reaction profiles of the gas-phase reactions do not resemble the related ones in a polar solvent.^{14,15} This is also found by the present study. Already if only bulk effects of a polar solvent are accounted for (entry 2 of Table 1, Figure 3B), the reaction barriers (15–16 kcal mol⁻¹) and also the energies of the products increase with respect to the reactants (4–10 kcal mol⁻¹). The reactants are more strongly stabilized by a polarizable environment than the TSs since in the former the charge is more localized than in the latter. Please note that within a polar solvent all IMCs are higher in energy than the reactants and do no longer represent stationary points on the potential energy surface.

For the epoxide system the reaction energy changes only by about 4 kcal mol⁻¹ if bulk effects are included while for the thiirane a change of nearly 10 kcal mol⁻¹ is found. For the aziridine the reaction energy increases from about +5 kcal mol⁻¹ to +11 kcal mol⁻¹. These differences can be rationalized by the different charge distributions of the products. In the product of the epoxide reaction, the charge is mainly concentrated on

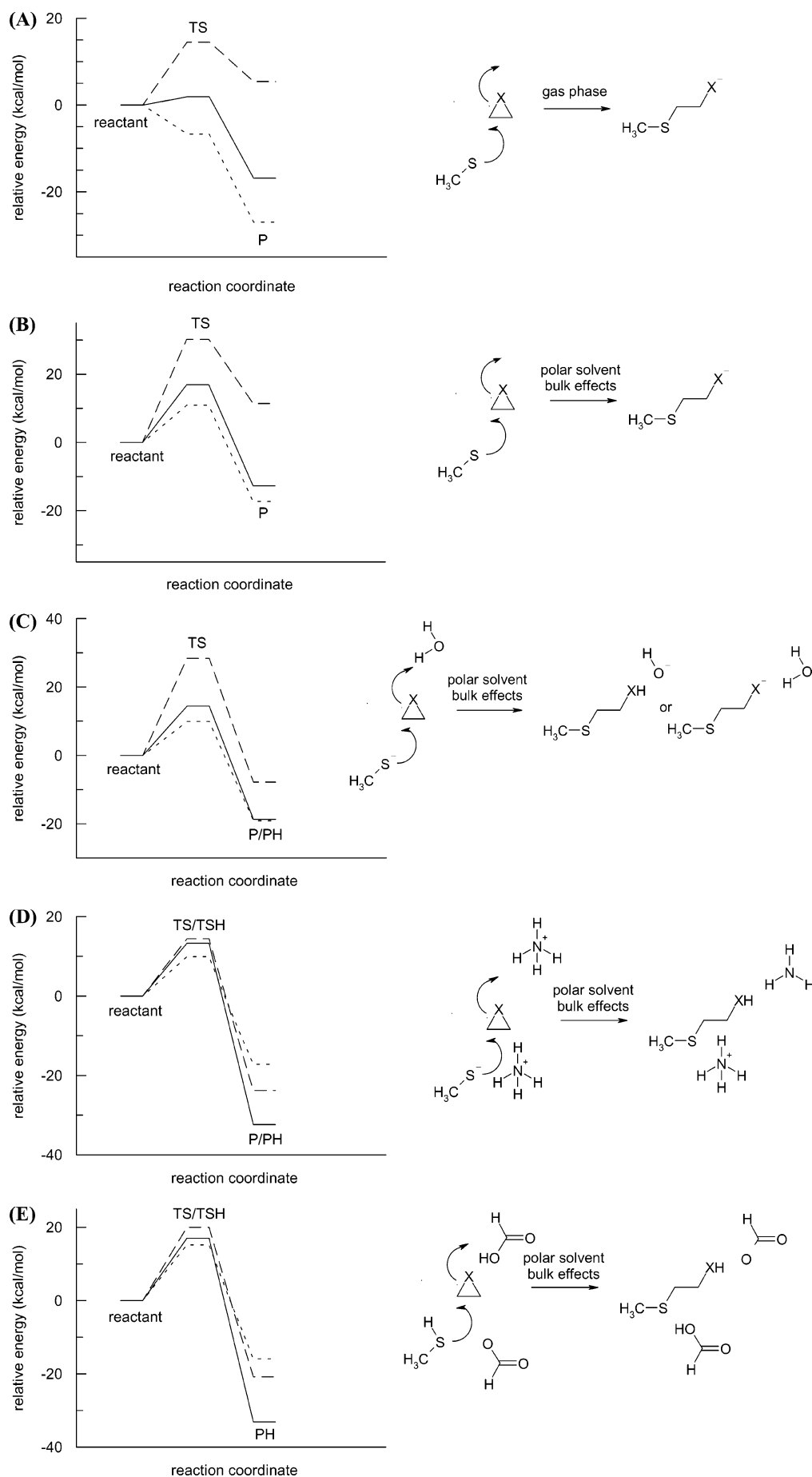


Figure 3. Relative energies for the model reactions of oxirane (—), aziridine (---), and thiirane (- - -) with methyl thiolate according to Table 1: (A) entry 1 (gas phase); (B) entry 2 (bulk effects); (C) entry 3 (1 H₂O); (D) entry 6 (2 NH₄⁺); (E) entry 8 (2 HCO₂H).

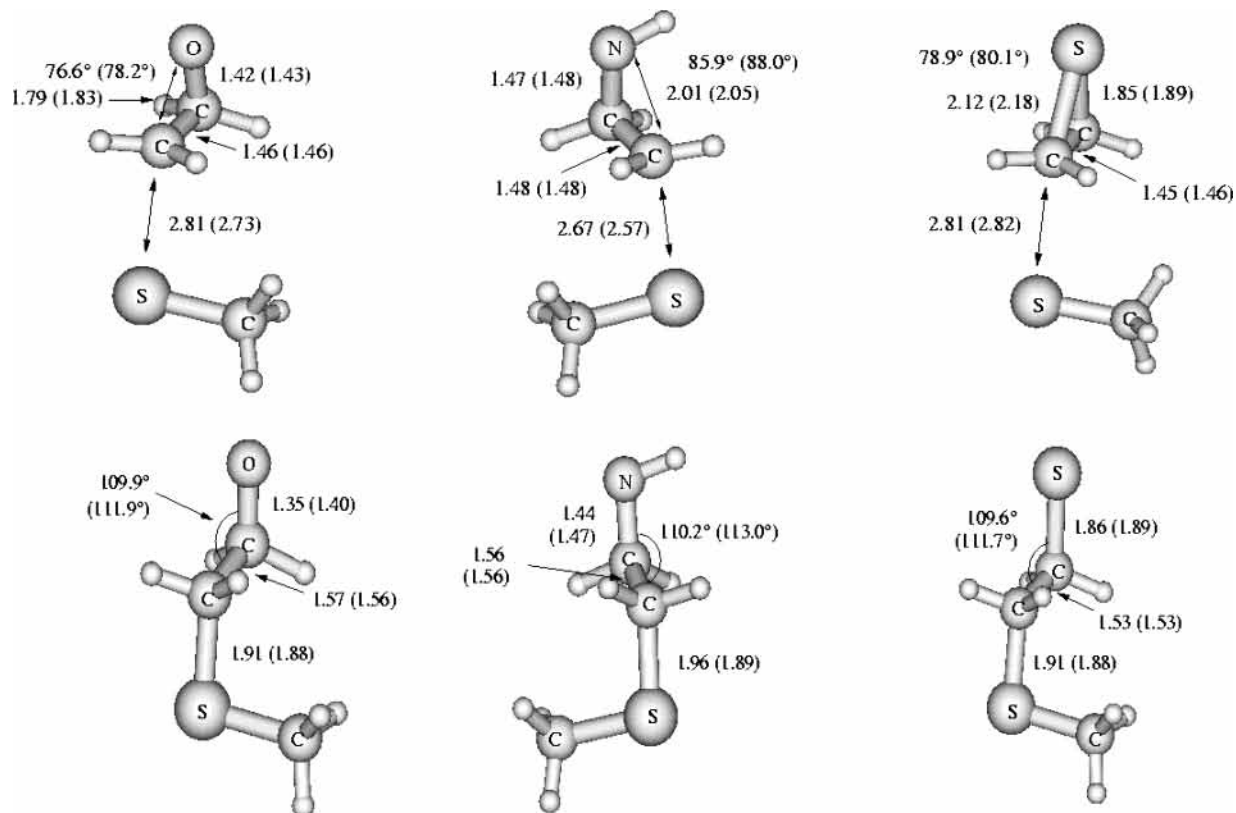


Figure 4. Geometrical arrangements of the transition states (TSs, upper row) and products (P, lower row) of the gas phase computations (entry 1 of Table 1). The geometrical values obtained if only bulk effects of water as solvent are considered (entry 2 of Table 1) are given in brackets. For more information see text.

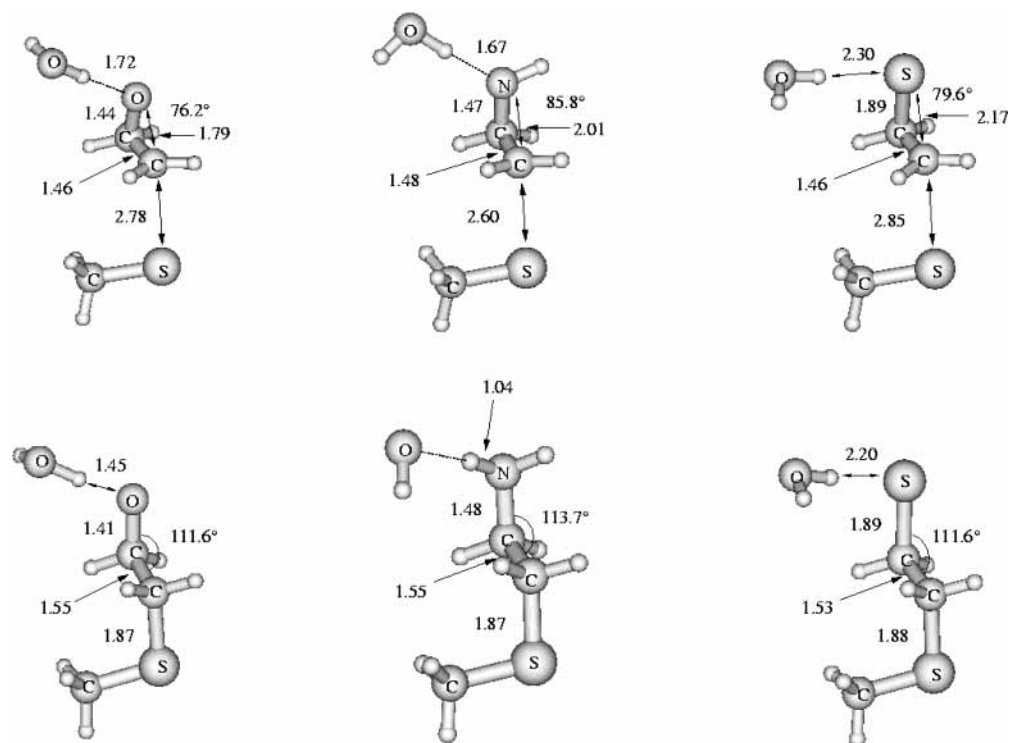


Figure 5. Geometrical arrangements of TSs (upper row) and products (lower row) employing the H₂O/- model (entry 3 of Table 1). For more information see text.

the oxygen center, which means that for reactants and products the charge is mainly localized on one center. Consequently, reactants and products are similarly influenced by a polarizable medium. For the product of the thiirane reaction the charge is

more delocalized (two sulfur centers) which explains the stronger energy rise of the products with respect to the reactants.

Comparing entry 1 (gas phase) and entry 2 (polar solvent) of Table 1, it becomes obvious that only the absolute values

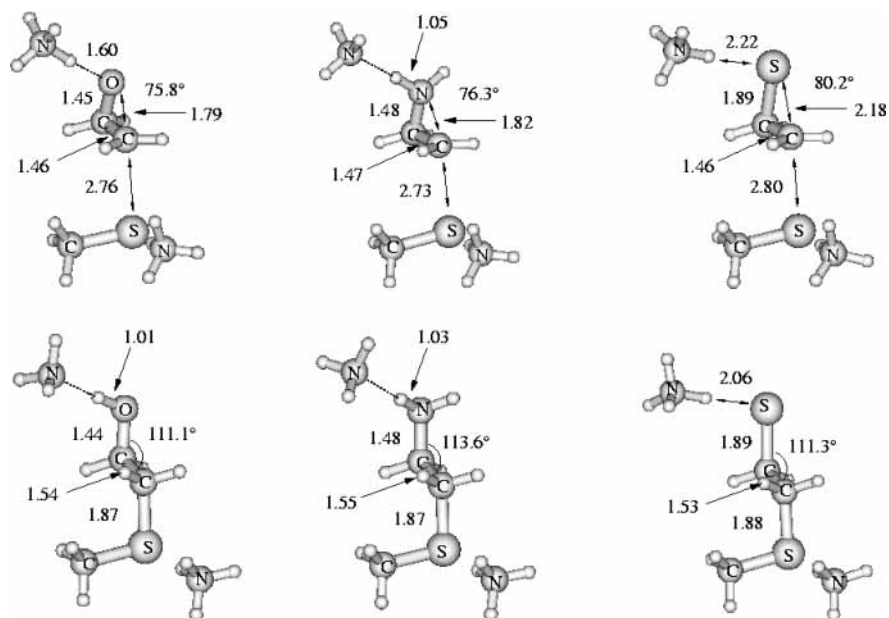


Figure 6. Geometrical arrangements of TSs (upper row) and products (lower row) for the $\text{NH}_4^+/\text{NH}_4^+$ model (entry 6 of Table 1).

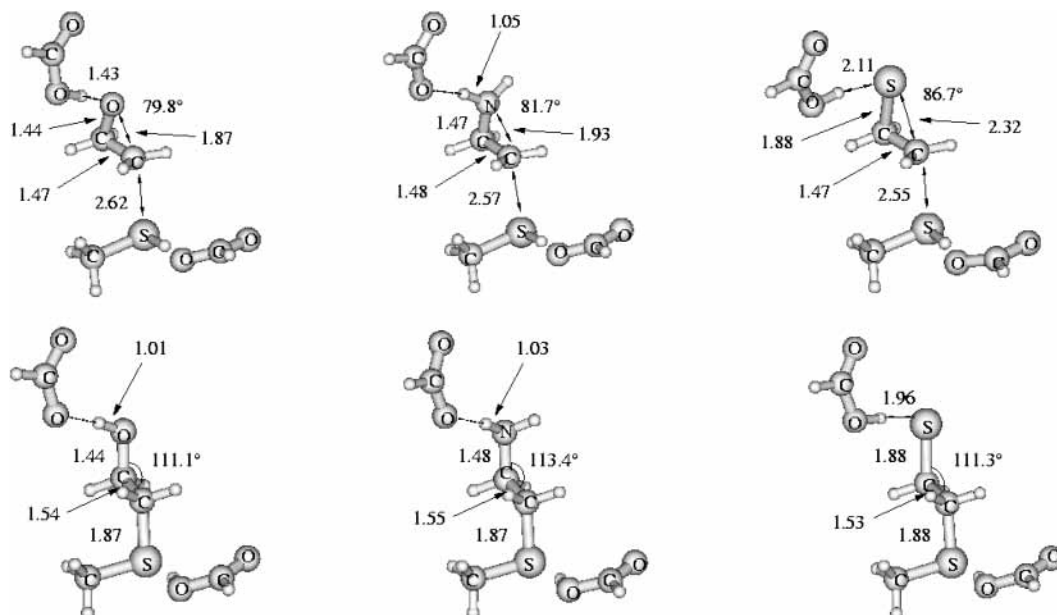


Figure 7. Geometrical arrangements of TSs (upper row) and products (lower row) for the $\text{HCO}_2\text{H}/\text{HCO}_2^-$ model (entry 8 of Table 1).

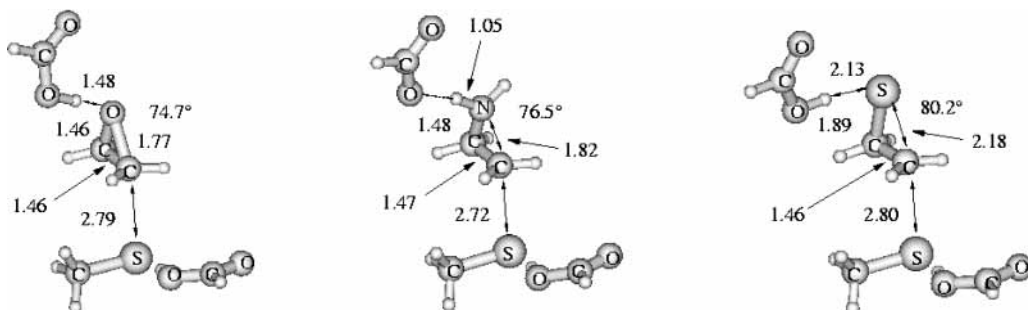


Figure 8. Geometrical arrangements of TSs for the $\text{HCO}_2\text{H}/\text{HCO}_2\text{H}$ model (entry 9 of Table 1). The products of the reactions are identical those which are given in Figure 7 ($\text{HCO}_2\text{H}/\text{HCO}_2^-$ model).

change while the order of activation energy and reaction energy found in the gas-phase remains.

If one water molecule (energies in entry 3 of Table 1, Figure 3C, geometrical arrangements in Figure 5) is included to account for molecular effects of the physiological medium, kinetics and

thermodynamics of the thiirane reaction change only slightly because the water molecule only acts as a solvent molecule; e.g., no proton transfer occurs, which is in line with the pK_a values of a thiol ($\approx 8-10$) and water ($=15.74$). For the epoxide system no proton transfer is found either but with respect to

TABLE 2: Enthalpy (ΔH_{298}) and Free Energy (ΔG_{298}) of the Reaction Profiles of the Ring Opening Reactions

	solvent molecules		epoxide			aziridine			thiirane		
			TS	P	PH	TS	TSH	PH	TS	P	PH
entry 1	H ₂ O/H ₂ O	ΔH_{298}	+15.5	-16.6		+28.8		-4.0	+11.5	-15.0	
		ΔG_{298}	+24.9	-3.9		+40.9		+5.8	+20.7	-3.9	
entry 2	NH ₄ ⁺ /H ₂ O	ΔH_{298}	+12.6		-34.9		+14.3	-25.1	+9.8	-18.7	-19.4
		ΔG_{298}	+22.8		-23.8		+24.4	-14.5	+18.2	-8.1	-9.1
entry 3	HCO ₂ H/H ₂ O	ΔH_{298}	+12.6		-35.5		+15.6	-22.9	+10.7	-17.8	-19.7
		ΔG_{298}	+22.8		-25.0		+25.3	-15.8	+20.4	-6.2	-9.9

^a All values are in kcal mol⁻¹. For more information see text.

TABLE 3: Influence of the Theoretical Approach on the Reaction Profiles of the Gas Phase Reactions^a

	epoxide			aziridine			thiirane		
	IMC	TS	P	IMC	TS	P	IMC	TS	P
BLYP	-6.5	-2.2	-17.6	-12.2	+8.6	+3.1	-8.8	<i>b</i>	-25.4
BPW91	-6.1	-0.8	-17.8	-12.6	+10.7	+3.7	-8.2	-7.9	-25.8
B3LYP	-6.7	+1.9	-16.9	-12.6	+14.5	+5.4	-8.1	-6.7	-27.0
^c B3LYP//BLYP	-6.7	+1.6	-16.9	-12.5	+14.4	+6.1	-7.8	<i>b</i>	-26.9
B3PW91	-6.4	+3.0	-17.0	-12.7	+16.1	+6.1	-7.7	-5.8	-27.2
MP2/aug-cc-pVDZ	<i>d</i>	+0.3	-21.2	<i>d</i>	+12.3	0.0	<i>d</i>	-7.6	-31.5
MP2/aug-cc-pVTZ	<i>d</i>	+2.3	-20.3	<i>d</i>	+14.0	+0.4	<i>d</i>	-5.7	-30.2
CCSD(T)/aug-cc-pVDZ	<i>d</i>	-0.2	-20.7	<i>d</i>	+11.3	+0.1	<i>d</i>	-8.5	-31.9
CCSD(T)/aug-cc-pVTZ ^e	<i>d</i>	+1.8	-19.8	<i>d</i>	+13.0	+0.5	<i>d</i>	-6.6	-30.6

^a All DFT based computations were performed with a 6-311+G(d) basis for the heavier centers while a 6-31G(p) basis was employed for the hydrogen centers. The basis sets used for the MP2 or CCSD(T) computation are explicitly given. All values are given in kcal mol⁻¹. For more information, see text. ^b The TS could not be located. ^c Single point calculations with the B3LYP functional. The geometry optimization were performed with the BLYP functional. ^d Not calculated. ^e Estimate based on the MP2 correction, i.e., E(CCSD(T)/aug-cc-pVTZ) = E(CCSD(T)/aug-cc-pVDZ) + {E(MP2/aug-cc-pVTZ) - E(MP2/aug-cc-pVDZ)}. For more information, see text.

TABLE 4: Comparison of Various Approaches for the Description of Solvent Effects of a Polar Solvent^a

	epoxide			aziridine			thiirane		
	IMC	TS	P	TS	P	PH	IMC	TS	P
Model I									
COSMO	+5.1	+14.4	-15.8	+27.7	+12.3		+8.3	<i>b</i>	-15.2
PCM	+9.4	+20.9	-3.7	+30.7	+18.3		+9.8	<i>b</i>	-4.2
IEF	+3.9	+13.0	-16.5	+26.6	+11.8		+6.8	<i>b</i>	-16.1
Model II									
COSMO	<i>b</i>	+12.8	-15.1	<i>b</i>	<i>b</i>	-13.1	+4.7	+10.1	-16.4
PCM	<i>b</i>	+11.6	-9.7	<i>b</i>	<i>b</i>	+6.9	+3.6	+7.6	-7.7
IEF	<i>b</i>	+11.1	-17.2	<i>b</i>	<i>b</i>	-16.9	+8.4	+8.3	-18.1
Model III									
COSMO	<i>b</i>	+12.5	-15.0	+24.5	<i>b</i>	-15.6	<i>b</i>	+10.8	-15.6
PCM	<i>b</i>	+13.4	-14.0	+27.2	<i>b</i>	+3.6	<i>b</i>	+13.4	-7.1
IEF	<i>b</i>	+11.7	-15.9	+23.9	<i>b</i>	-15.3	<i>b</i>	+9.8	-16.2
I-PCM	<i>b</i>	+11.9	<i>b</i>	+24.4	<i>b</i>	-11.8	<i>b</i>	+9.2	<i>b</i>

^a In model I the influence of the solvent is only accounted for by various continuum approaches, i.e., no water is explicitly taken into account. For all approaches the standard settings of the GAUSSIAN98 were employed. In model II molecular effects of a water environment are modeled by one water molecule which is placed in the vicinity of the heteroatom X of the ring. In model III an additional water molecule is positioned in the neighborhood of the sulfur center of the methyl thiolate. The geometries of the water molecules are fully optimized. All calculations are single point computations with the BLYP functional in combination with 6-311+G(d) basis sets. The geometries were taken from a BLYP computation employing a TZV + P basis set in combination with the COSMO approach. For more information see text. All values are given in kcal mol⁻¹. ^b The stationary point could not be located.

the situation before the absolute value of the reaction energy is decreased by 6–7 kcal mol⁻¹ to about -18 kcal mol⁻¹. Please note that computations with the standard COSMO settings in the GAUSSIAN predict a proton transfer for the products leading to stabilized products. Further computations were not possible due to problems in geometry optimization.

For the aziridine system the reaction energy drops dramatically. While the reaction is predicted to be endothermic (+11.4 kcal mol⁻¹) if only bulk effects of the solvent are taken into account an exothermic reaction (-7.8 kcal mol⁻¹) is computed if one water molecule is placed in the vicinity of nitrogen center. The reason for this dramatic change is a proton transfer from the water molecule to the NRH⁻ unit of the product (Figure 5). Please note that with the use of the standard parameters setting

of the GAUSSIAN program the computations predict an even lower reaction energy of about -14 kcal mol⁻¹ (see Table 5, model II or III), which is comparable to those of the epoxide or thiirane reactions.

While the reaction energy changes considerably the reaction barrier of the aziridine ring opening stays around 28 kcal mol⁻¹. This is in line with the finding that for the TS the water molecule in the vicinity of the NH group only acts as a solvent molecule. Also all other barrier heights only change slightly if in addition to bulk effects one water molecule is explicitly considered. Therefore, the order $\Delta E^\ddagger(\text{thiirane}) < \Delta E^\ddagger(\text{epoxide}) \ll \Delta E^\ddagger(\text{aziridine})$ remains.

If a second water molecule is placed near the sulfur center of the methyl thiolate to include molecular solvent effects arising

TABLE 5: Influence of the Parameters Used for the COSMO Approach on the Reaction Profiles of the Aziridine Ring Opening^a

	TS	P	PH
gas phase	+8.6	+3.1	
	Model I		
GAUSSIAN	+27.7	+12.3	
TURBOMOLE	+25.0	+10.8	
	Model II		
GAUSSIAN	<i>b</i>	<i>c</i>	-13.1
TURBOMOLE	+23.5	<i>c</i>	-7.5
	Model III		
GAUSSIAN	+24.5	<i>c</i>	-15.6
TURBOMOLE	+23.2	<i>c</i>	-6.0
	Model IV		
GAUSSIAN	<i>c</i>	<i>c</i>	-6.9
TURBOMOLE	+22.8	<i>c</i>	-12.0

^a GAUSSIAN denotes that the standard parameter values of the GAUSSIAN98 program package were used. TURBOMOLE indicates the use of the standard TURBOMOLE parameters which agree with the original values suggested by Klamt and Schuurmann.²² For both computations ϵ was set to 78.39. For GAUSSIAN a 6-311+G(d) basis set was employed while a TZV+P basis set was used for the TURBOMOLE computations. The BLYP functional was used in both sets of computations. The geometries were taken from the TURBOMOLE computations. In model IV two water molecules are positioned in the vicinity of the NH unit of the aziridine but none in the vicinity of the sulfur center of the thiolate. ^b The stationary point could not be located. ^c Not calculated.

around the thiolate anion (entry 4 of Table 1) only very small changes are found in all cases. Also the relevant geometrical parameters are nearly identical to those shown in Figure 5.

Placing an NH_4^+ molecule instead of a water molecule in the vicinity of the NH group of the aziridine (entry 5 of Table 1) the computed reaction barrier of the ring opening reaction decreases dramatically (12.9 vs 28.3 kcal mol⁻¹). The reason for this remarkable change is the protonation of the emerging NH^- unit already at the transition state. Also the reaction energy is lowered from around -7 to -27 kcal mol⁻¹ if catalysis by an NH_4^+ molecule is considered. The relevant geometrical parameter can be taken from Figure 6. Figure 6 depicts the situation for the $\text{NH}_4^+/\text{NH}_4^+$ model but the relevant parameters of both models are very similar. The reaction barrier of the epoxide reaction is computed to be 11.8 kcal mol⁻¹, which is about 2–3 kcal mol⁻¹ lower than the barrier found with one water molecule alone. Please note that the decrease of the barrier takes place although the TS is not protonated. The reaction energy decreases strongly to about -35 kcal mol⁻¹ which is due to proton transfer from the NH_4^+ to the alcoholat yielding an alcohol. For the thiirane system only small changes are found. We also located the protonated product (thiol instead of thiolate), but it was computed to be only somewhat lower in energy.

If the catalysis from a proton source such as NH_4^+ is taken into account, the reaction barrier of the aziridine reaction becomes comparable to the one of the epoxide reaction. This difference to the situation with two water molecules as catalyst underlines the strong influence of a proton source on the relative reaction velocities. For the thermodynamics such a proton source even reverses the order: while ΔE_R (epoxide) \cong ΔE_R (thiirane) \ll ΔE_R (aziridine) is found for environments without an effective proton source, ΔE_R (epoxide) \leq ΔE_R (aziridine) \ll ΔE_R (thiirane) is computed if a proton source like NH_4^+ is available. Influences of the NH_4^+ could also result since it represents a charged species.²⁵ However, a comparison to the

corresponding systems (e.g., with HCO_2H as proton donor for the epoxide system the same activation barrier is computed, see below) indicates that this effect is small.

In the $\text{NH}_4^+/\text{NH}_4^+$ model (entry 6 of Table 1, Figure 6, Figure 3D) a second NH_4^+ molecule is placed in the vicinity of the attacking methyl thiolate, i.e., also the attacking methyl thiolate “feels” the lower pH value. With respect to the $\text{NH}_4^+/\text{H}_2\text{O}$ model, our computations predict a slight rise of the barriers (1–2 kcal mol⁻¹) for all systems. These only minor changes arise because no protonation of the methyl thiolate is found, i.e., the NH_4^+ acts as a normal solvent molecule.

To mimic an even higher proton donor ability of the environment we used formic acid ($\text{p}K_a \approx 3.8$). Comparing the $\text{HCO}_2\text{H}/\text{H}_2\text{O}$ model (entry 7 of Table 1) with the $\text{NH}_4^+/\text{H}_2\text{O}$ model nearly no differences are found for the epoxide. For the aziridine the proton donor ability of HCO_2H is sufficient to protonate the reactants (Figure 7, 8). However, despite the expected increased electrophilicity of the protonated aziridine the reaction barrier increases slightly with respect to the $\text{NH}_4^+/\text{H}_2\text{O}$ model (1–2 kcal mol⁻¹). Also for thiiranes a small increase of the barrier (1–2 kcal mol⁻¹) is predicted. Please note that despite the strong proton donor ability of HCO_2H only the TS of the aziridine reaction is protonated while the TS of the epoxide and thiirane remains unprotonated.

For the epoxide our computations for the $\text{HCO}_2\text{H}/\text{H}_2\text{O}$ model are in line with results of Laitinen et al., who studied the acid catalyzed opening of an epoxide with acetate as nucleophile and a second acetic acid as catalyst.¹⁵

Methyl mercaptan has a $\text{p}K_a$ value of ca. 9.8. As a consequence a proton transfer should take place from the formic acid molecule to the attacking thiolate if the acid molecule is placed in its vicinity. We indeed find that the ($\text{HCO}_2^- + \text{H}_3\text{CSH}$)-form is more stable by about 3 kcal mol⁻¹ than the ($\text{HCO}_2\text{H} + \text{H}_3\text{CS}^-$)-form, however. Both represent minima on the potential energy surface. In Table 1 the computations which start from the lower-in-energy ($\text{HCO}_2^- + \text{H}_3\text{CSH}$)-form are given as $\text{HCO}_2\text{H}/\text{HCO}_2^-$ (entry 8 of Table 1, Figure 3 E). Along the reaction path the H_3CS -unit stays protonated (Figure 7), i.e., also at the TS a protonated thiol unit is found. As expected, in the products the proton moves back from the H_3CS -unit to the formic acid (Figure 7). In comparison with the $\text{HCO}_2\text{H}/\text{H}_2\text{O}$ model all barrier heights increase by about 5–6 kcal mol⁻¹ and also the reaction energies indicate less exothermic reactions (4–5 kcal mol⁻¹). The increase in the barrier is understandable because the thiol is a less efficient nucleophile than the deprotonated thiolate. Our results explain the experimental observations of Meara and Rich,⁷ who found a strong decrease of k_i at decreasing pH values and connected it to the protonation of an acidic group possessing a $\text{p}K_a$ of about 4. Our calculations indicate that this group is the thiolate of the attacking cysteine.

Indeed, for the active site in cysteine proteases it could be shown that the deprotonated cysteine is strongly stabilized leading to a $\text{p}K_a$ value of about 4, which is only slightly higher than the $\text{p}K_a$ value of formic acid. To mimic the reaction of a still deprotonated cysteine within a quite acid environment we also computed the reaction starting from the ($\text{HCO}_2\text{H} + \text{H}_3\text{CS}^-$)-form (entry 9 of Table 1, Figure 8). Along this reaction path the methyl thiolate remains deprotonated also at the TS but both reaction paths, $\text{HCO}_2\text{H}/\text{HCO}_2^-$ and $\text{HCO}_2\text{H}/\text{HCO}_2\text{H}$, end in the same products. For the unprotonated methyl mercaptan our computations predict lower barriers (ca. 5 kcal mol⁻¹) for all systems underlining the expected higher reactivity of the thiolate.

Comparing HCO_2H and NH_4^+ as proton sources (Table 1, entries 5 and 7), the increased donor ability of HCO_2H seems to slow the aziridine and thiirane reactions to a small extent while no change is found for the epoxide. A protonation of the methyl thiolate (entry 8) influences all reactions in a similar manner so that again no changes in the trends are observed.

Estimation of Entropy Effects

In the present study, differences between the alkylation steps of the epoxide, aziridine and thiirane inhibition mechanisms were studied on the basis of relative energies; i.e., entropy effects were not taken into account.

Table 2, which lists the computed ΔH and ΔG values for some of the present model reactions, seems to indicate a tremendous influence of entropy effects. With respect to the activation energies (Table 1) the free activation energies are much larger and the computed absolute values of the free reaction energies (Table 2) are smaller than the corresponding reaction energy values in Table 1. The entropy effects are quite uniform for all reactions. A closer inspection, however, shows that the entropy effects mainly influence the reaction profiles only up to the TSs. While the barriers increase considerably the free energy differences between the TSs and the products are very similar to the corresponding energy values. This indicates that the major part of the entropy effects stems from the loss of the rotational and translation degrees of freedom due to the association process. Relating this finding with the two step model (eq 1) assumed for the inhibition mechanism of irreversible inhibitors containing electrophilic warheads, it becomes clear that the entropy effects given in Table 2 influence the dissociation constant K_i rather than the first-order rate constant k_i , which is the topic of the present work; i.e., a comparison on the basis of energy differences is better suited for our question.

The values in Table 2 do not include entropy effects arising from reorganization of the water shell which are known to dominate total entropy effects for reactions of charged systems.²⁶ An accurate determination of such effects is difficult but for the present study qualitative considerations are already quite informative. Because of the strong basicity of the emerging NH^- unit of the aziridine system both TS and product become already protonated by weak proton sources. For epoxide and thiirane, we only predict the protonation of the product. Since such protonations neutralize the reacting system, it will lead to a less ordered solvent shell. The resulting entropy effects are positive; i.e., they should favor the ring opening. For aziridines these effects will lower already the barrier while for both other systems only the reaction energies will become more favorable.

Assessment of the Accuracy of Employed Theoretical Approaches

Gas-phase results computed with various quantum chemical approaches are summarized in Table 3. All DFT based computations were performed with a 6-311+G(d) basis²⁷ for the heavier centers while a 6-31G(p) basis²⁷ was employed for the hydrogen centers. The AO basis sets include diffuse functions for all heavier centers to ensure a reliable description of the negative charged centers. In line with findings in the literature,²⁸ hybrid functionals tend to predict higher reaction barriers than pure gradient corrected ones (3–6 kcal mol⁻¹). The reaction energies depend less on the chosen functional (1–2 kcal mol⁻¹). Differences between the MP2/cc-pVDZ and the corresponding CCSD(T) results²⁹ are even smaller (≤ 1 kcal mol⁻¹). Within the MP2 approach,²⁹ somewhat higher reaction

barriers and energies (≈ 1 –2 kcal mol⁻¹) are predicted if instead of the aug-cc-pVDZ³⁰ the more flexible aug-cc-pVTZ basis is used. CCSD(T) computations in combination with the larger aug-cc-pVTZ basis set were not feasible. Therefore, to estimate the difference between MP2/aug-cc-pVDZ and MP2/aug-cc-pVTZ computation to the CCSD(T)/aug-cc-pVDZ result. A comparison of these methods with the DFT approaches shows that the barrier heights obtained with the B3LYP/6-311+G(d) approach agree astonishingly good with the CCSD(T)/aug-cc-pVTZ approach while the predictions of the hybrid functional BLYP are 4–5 kcal mol⁻¹ lower. Since the RI (resolution of identity)³¹ ansatz allows a very efficient implementation for pure gradient corrected functionals we tested if the BLYP functional is accurate enough for the determination of the geometries. Indeed Table 3 shows that relative energies obtained by single point calculations with the B3LYP functional employing the BLYP geometries (in Table 3 abbreviated as B3LYP//BLYP) are also in line with the CCSD(T) results (deviations of about 1 kcal mol⁻¹). Please note that the B3LYP//BLYP approach underestimates the exothermicity of the reactions (3–6 kcal mol⁻¹).

For various ring-opening reactions of epoxides with nucleophiles, it could be shown that the influence of a polar solvent is tremendous.^{14,15} Therefore, a careful analysis of the accuracy of the various theoretical approaches was performed. The results are summarized in Table 4. Many effects of a polar solvent can already be accounted for if the solvent is described as a polarizable continuum (bulk effects).³² To determine the most appropriate continuum approach we tested the COSMO (conductor-like screening model),²² the PCM (polarizable continuum model)³³ and the more general IEF-PCM (integral equation formalism polarizable continuum model),³⁴ which contains both former approaches as limiting cases. In Table 4 these computations are summarized as model I (corresponding to entry 2, Table 1). Nonlinear effects, which arise from the molecular nature of the solvent, were investigated by placing one water molecule in the vicinity of the heteroatom of the ring (model II, corresponding to entry 3, Table 1) and an additional water molecule in the neighborhood of the sulfur center of the methyl thiolate, respectively (model III, corresponding to entry 4, Table 1). The geometries of the water molecules were fully optimized. In these calculations, bulk effects were also accounted for. For model III we also tested the I-PCM model (isodensity surface polarized continuum model).³⁵ In all calculations, the geometries were optimized within the given approach. Since all functionals showed comparable trends we focused on the BLYP functional. Please note that the values of Table 1 and Table 4 do not agree completely since the ones of Table 1 are computed with the B3LYP functional while the BLYP functional was used for Table 4. All trends are identical, however.

A comparison of the different theoretical approaches in Table 4 shows that the COSMO and the IEF-PCM approach agree quite nicely while the PCM predicts considerably higher reaction barriers and less exothermic reactions. For epoxide and thiirane a test of the reliability of the various approaches is possible by considering the influence of the additional water molecules (model II and III) on the activation barriers or the reaction energies. The influence should be small since the water molecules only act as solvent molecules. Table 4 indeed shows that the COSMO and the IEF-PCM ansatz do not change considerably if the number of explicit solvent molecules increases (≤ 2 kcal mol⁻¹). For PCM, the computed reaction barriers and the reaction energies strongly depend on the number of explicit water molecules. The superiority of COSMO or IEF-

PCM against PCM is also supported by the results from the I-PCM approach.

Within the calibration of the theoretical approaches we always compared standard single point computations performed with GAUSSIAN98 with standard single point computations employing TURBOMOLE to test the robustness of the theoretical description. Such test calculations seem to be important since continuum approaches often fail if charged systems are involved.^{31,32} Standard GAUSSIAN98 calculation means that we used a 6-311+G(d) basis for the heavier centers in combination with the standard parameters of the GAUSSIAN98 program package for the COSMO or for the other approaches.³⁶ Standard TURBOMOLE denotes that we used a TZV+P basis set in combination with the standard parameters of the COSMO approach within the TURBOMOLE program package.³⁷ The differences between both approaches should be small since the quality of both basis sets is similar. Indeed for the epoxide and the thiirane model (data not shown) the deviations are within the expected range (1–3 kcal mol⁻¹). For the aziridine system, however, large differences arise for the reaction energy of model II (-13 vs -7 kcal mol⁻¹) and III (-16 vs -6 kcal mol⁻¹) as can be seen from Table 5 which summarizes the values computed for the aziridine system. For model I (no additional water molecule) both approaches agree nicely. The analysis shows that the differences are connected with the hydroxyl anion, which arises during the proton transfer from the water molecule to the NH⁻ unit. To check the convergence of both parameter settings with respect to the number of explicitly included water molecules we placed another water molecule in the vicinity of the hydroxyl unit (model IV). For this model the GAUSSIAN98 settings give a reaction energy of about -7 kcal mol⁻¹ while the TURBOMOLE settings give a value around -12 kcal mol⁻¹. This shows that both parameter sets have drawbacks and that more explicit water molecules are necessary for a converged description of the hydroxyl anion.

Summary

The present study indicates that the influence of the environmental pH value on the inhibition potency of epoxide, aziridine, or thiirane based cysteine protease inhibitors is in parts connected with changes in the kinetics and the thermodynamics of the alkylation step. For aziridines, weak proton donors lead to strongly decreased reaction barriers and considerably more exothermic reactions. For epoxides, only the thermodynamics become more favorable while the reaction barriers are only slightly influenced. For thiiranes, no catalysis is found. This becomes obvious by Figure 3.

The aziridine inhibition mechanism (association and alkylation step) will additionally be favored with respect to both other ones by entropy effects connected with reorganization of the solvent shell. They arise because the negative charged species become neutral due to protonation.

Finally our study suggests that the decrease in the k_i values of the epoxide reaction found for low pH values is a result of protonation of the attacking cysteine. For example, in our model the interaction of NH₄⁺ with the attacking methyl thiolate increases the reaction barrier by about 1–2 kcal mol⁻¹ if no proton transfer occurs. If the thiolate moiety is protonated (e.g., by the stronger proton donor formic acid) the reaction barrier increases by about 5 kcal mol⁻¹.

Acknowledgment. This work was funded by the DFG (Deutsche Forschungsgemeinschaft) in the framework of the SFB 630 Recognition, Preparation and Functional Analysis of Agents against Infectious Diseases.

Supporting Information Available: Table of the absolute values of the energies and the Cartesian coordinates of the B3LYP/TZV+P // BLYP/TZV+P computations. This material is available free of charge via the Internet at <http://pubs.acs.org>.

References and Notes

- (1) (a) Broemme, D.; Kaleta, J. *Curr. Pharm. Des.* **2002**, *8*, 1639–1658. (b) McGrath, M. E. *Annu. Rev. Biophys. Biomol. Struct.* **1999**, *28*, 181–204. (c) Otto, H.-H.; Schirmeister, T. *Chem. Rev.* **1997**, *97*, 133–171. (d) Powers, J. C.; Asgian, J. L.; Ekici, O. D.; James, K. E. *Chem. Rev.* **2002**, *102*, 4639–750. (e) Leung-Toung, R.; Li, W.; Tam, T. F.; Karimian, K. *Curr. Med. Chem.* **2002**, *9*, 979–1002. (f) Lecaille, F.; Kaleta, J.; Broemme, D.; *Chem. Rev.* **2002**, *102*, 4459–4488.
- (2) Schirmeister, T.; Klockow, A. *Mini Rev. Med. Chem.* **2003**, *3*, 6, 585–596.
- (3) Hanada, K.; Tamai, M.; Yamagishi, M.; Ohmura, S.; Sawada, J.; Tanaka, I.; *Agric. Biol. Chem.* **1978**, *42*, 523–528.
- (4) (a) Schirmeister, T. *Arch. Pharm. Pharm. Med. Chem.* **1996**, *329*, 239–244. (b) Schirmeister, T. *J. Med. Chem.* **1999**, *42*, 560–572. (c) Schirmeister, T.; Peric, M. *Bioorg. Med. Chem.* **2000**, *8*, 1281–1291. (d) Martichonok, V.; Plouffe, C.; Storer, A. C.; Ménard, R.; Jones, B. *J. Med. Chem.* **1995**, *38*, 3078–3085. (e) Yamamoto, M.; Powers, J. C.; Tachibana, T.; Egusa, K.; Okawa, K. *Pept. Chem.* **1993**, 189–192.
- (5) (a) Schirmeister, T. *Bioorg. Med. Chem. Lett.* **2000**, *10*, 2647–2651; (b) Bruno, G.; Schirmeister, T. *Arch. Pharm. Pharm. Med. Chem.* **2004**, *337*, 90–95.
- (6) Kumar, J. S. R.; Roy, S.; Dutta, A. *Bioorg. Med. Chem. Lett.* **1999**, *9*, 513–514.
- (7) Meara, J. P.; Rich, D. H. *J. Med. Chem.* **1996**, *39*, 3357–3366.
- (8) Bihovsky, R.; Powers, J. C.; Kam, C.-M.; Walton, R.; Loew, R. C. *J. Enzyme Inhib.* **1993**, *7*, 15–25.
- (9) Tamai, M.; Adachi, T.; Oguma, K.; Morimoto, S.; Hanada, K.; Ohmura, S.; Ohzeki, M. *Agric. Biol. Chem.* **1981**, *45*, 675–679.
- (10) Bihovsky, R. *J. Org. Chem.* **1992**, *57*, 1029–1031.
- (11) Rich, D. H.; Inhibitors of Cysteine Proteases. In *Proteinase Inhibitors*; Barrett, A. J., Salvesen, G. S., Eds.; Elsevier Science Publishers B.V.: Amsterdam, 1986; pp 153–178.
- (12) (a) Varughese, K. L.; Ahmed, F. R.; Carey, P. R.; Hasnain, S.; Huber, C. P.; Storer, A. C. *Biochemistry* **1989**, *28*, 1330–1332. (b) Varughese, K. L.; Su, Y.; Cromwell, D.; Hasnain, S.; Xuong, N. H. *Biochemistry* **1992**, *31*, 5172–5176. (c) Katerelos, N. A.; Taylor, M. A.; Scott, M.; Goodenough, P. W.; Pickersgill, R. W. *FEBS Lett.* **1996**, *392*, 35–39. (d) Bhattacharya, S.; Ghosh, S.; Chakraborty, S.; Bera, A. K.; Mukhopadhyay, B. P.; Dey, I.; Banerjee, A. *BMC Struct. Biol.* **2001**, *1*, 4–20. (e) Yamamoto, A.; Tomoo, K.; Matsugi, K.; Hara, T.; In, Y.; Murata, M.; Kitamura, K.; Ishida, T.; *Biochim. Biophys. Acta* **2002**, *1597*, 244–251. (f) Zhao, B.; Janson, C. A.; Amegadzie, B. Y.; D'Alessio, K.; Griffin, C.; Hanning, C. R.; Jones, C.; Kurdyla, J.; McQueney, M.; Qiu, X.; Smith, W. W.; Abdel-Meguid, S. S.; *Nat. Struct. Biol.* **1997**, *4*, 109–111. (g) Yamamoto, D.; Matsumoto, K.; Ohishi, H.; Ishida, T.; Inoue, M.; Kitamura, K.; Mizuno, H. *J. Biol. Chem.* **1991**, *266*, 14771–14777. (h) Kim, M. J.; Yamamoto, D.; Matsumoto, K.; Inoue, M.; Ishida, T.; Mizuno, H.; Sumiya, S.; Kitamura, K. *Biochem. J.* **1992**, *287*, 797–803. (i) Fujishima, A.; Imai, Y.; Nomura, T.; Fujisawa, Y.; Yamamoto, Y.; Sugawara, T. *FEBS Lett.* **1997**, *407*, 47–50. (k) Matsumoto, K.; Murata, M.; Sumiya, S.; Mizoue, K.; Kitamura, K.; Ishida, T. *Biochim. Biophys. Acta* **1998**, *1383*, 93–100.
- (13) Moroder, L.; Musiol, H.-J.; Scharf, R. *FEBS Lett.* **1992**, *299*, 51–53.
- (14) Lau, E. Y.; Newby, Z. E.; Bruce, T. C. *J. Am. Chem. Soc.* **2001**, *123*, 3350–3357.
- (15) Laitinen, T.; Rouvinen, J.; Peräkylä, M. *J. Org. Chem.* **1998**, *63*, 8157–8162.
- (16) Schröder Glad, S.; Jensen, F. *J. Chem. Soc., Perkin Trans. 2* **1994**, 871–876.
- (17) Gronert, S.; Lee, J. M. *J. Org. Chem.* **1995**, *60*, 4488–4497.
- (18) Omoto, K.; Fujimoto, H. *J. Org. Chem.* **2000**, *65*, 2464–2471.
- (19) Banks, H. D.; White, W. E. *J. Org. Chem.* **2001**, *66*, 5981–5986.
- (20) Nielsen, I. M. B. *J. Phys. Chem. A* **1998**, *102*, 3193–3201.
- (21) Wolk, J. L.; Hoz, T.; Basch, H.; Hoz, S. *J. Org. Chem.* **2001**, *66*, 915–918.
- (22) Klamt, A.; Schüürmann, G. *J. Chem. Soc., Perkin Trans. 2* **1993**, 799–805.
- (23) (a) Becke, A. D. *J. Chem. Phys.* **1993**, *98*, 5648–5652; (b) Becke, A. D. *J. Chem. Phys.* **1993**, *98*, 1372–1377; (c) Lee, C.; Yang, W.; Parr, R. G. *Phys. Rev. B* **1988**, *37*, 785–789.
- (24) Schäfer, A.; Huber, C.; Ahlrichs, R. *J. Chem. Phys.* **1997**, *100*, 5829–5835.
- (25) Jencks, D. A.; Jencks, W. P. *J. Am. Chem. Soc.* **1977**, *99*, 7948–7960.

(26) Hoffmann, R. W. *Aufklärung von Reaktionsmechanismen*; Thieme: Stuttgart, Germany, 1976.

(27) (a) Hehre, W. J.; Ditchfield, R.; Pople, J. A. *J. Chem. Phys.* **1972**, *56*, 2257–2261; (b) Poirier, R.; Kari, R.; Csizmadia, I. G. *Handbook of Gaussian basis sets, Physical Science Data 24*; Elsevier: Amsterdam, 1985.

(28) Koch, W.; Holthausen, M. C. *A Chemist's Guide to DFT*; Wiley-VCH: Weinheim, Germany, 2001.

(29) Helgaker, T.; Jørgensen, P.; Olsen, J. *Molecular Electronic-Structure Theory*; Wiley: Chichester, England 2000.

(30) (a) Woon, D. E.; Dunning, T. H., Jr. *J. Chem. Phys.* **1993**, *98*, 1358–1371. (b) Kendall, R. A.; Dunning, T. H., Jr.; Harrison, R. J. *J. Chem. Phys.* **1992**, *96*, 6796–6806. (c) Wilson, C.; vanMourik, T.; Dunning, T. H., Jr. *J. Mol. Struct. (THEOCHEM)* **1997**, *388*, 339–349.

(31) Kendall, R. A.; Früchtl, H. A. *Theor. Chem. Acc.* **1997**, *97*, 158–163.

(32) (a) Cramer, C. J.; Truhlar, D. G. *Chem. Rev.* **1999**, *99*, 2161–2200. (b) Tomasi, J.; Persico, M. *Chem. Rev.* **1994**, *94*, 2027–2094.

(33) Aguilar, M. A.; Olivares del Valle, F. J.; Tomasi, J. *J. Chem. Phys.* **1993**, *98*, 7375–7384.

(34) Cancès, E.; Mennucci, B.; Tomasi, J. *J. Chem. Phys.* **1997**, *107*, 3032–3041.

(35) Foresmann, J. B.; Keith, T. A.; Wiberg, K. B.; Snoonian, J.; Frisch, M. J. *J. Phys. Chem.* **1996**, *100*, 16098–16104.

(36) Frisch, M. J.; Trucks, G. W.; Schlegel, H. B.; Scuseria, G. E.; Robb, M. A.; Cheeseman, J. R.; Zakrzewski, V. G.; Montgomery, J. A.; Stratmann, R. E.; Burant, J. C.; Dapprich, S.; Millam, J. M.; Daniels, A. D.; Kudin, K. N.; Strain, M. C.; Farkas, O.; Tomasi, J.; Barone, V.; Cossi, M.; Cammi, R.; Mennucci, B.; Pomelli, C.; Adamo, A.; Clifford, S.; Ochterski, J.; Petersson, G. A.; Ayala, P. Y.; Cui, Q.; Morokuma, K.; Malick, D. K.; Rabuck, A. D.; Raghavachari, K.; Foresman, J. B.; Cioslowski, J.; Ortiz, J. V.; Stefanov, B. B.; Liu, G.; Liashenko, A.; Piskorz, P.; Komaromi, I.; Gomperts, R.; Martin, R. L.; Fox, D. J.; Keith, T.; Al-Laham, M. A.; Peng, C. Y.; Nanayakkara, A.; Gonzalez, C.; Challacombe, M.; Gill, P. M. W.; Johnson, B. G.; Chen, W.; Wong, M. W.; Andres, J. L.; Head-Gordon, M.; Replogle, E. S.; Pople, J. A. *Gaussian 98 (Revision A.7)*; Gaussian, Inc.: Pittsburgh, PA, 1998.

(37) TURBOMOLE Vers. 5.3, Quantum Chem. Group, University of Karlsruhe, Germany, 1988.